ISSN 2176-5480

22nd International Congress of Mechanical Engineering (COBEM 2013)
November 3-7, 2013, Ribeirão Preto, SP, Brazil

THE INVERSE PIEZOELECTRIC EFFECTS ON THE AEROELASTIC STABILITY OF COMPOSITE SHELLS

Maurício V. Donadon
Alfredo R. de Faria
Sérgio F. M. de Almeida
Instituto Tecnológico de Aeronáutica-ITA
donadon@ita.br; arfaria@ita.br;frascino@ita.br

Abstract. *This work investigates the aeroelastic stability boundary of flutter in aircraft composite panels, curved or flat, subject to the effect of stress stiffening caused by the piezoelectric actuator (PZT). Hamilton's principle is used for the formulation of the energy functional and to obtain the equilibrium equations and boundary conditions of the problem. The finite element method is employed to numerically solve the equations. The aeroelastic behavior of panels manufactured in composite material (boron–epoxy) or conventional material (aluminum 2024-T3) are assessed. Two layers of piezoelectric material (ACX QP10N) are attached to the panels: one on the top surface one on the bottom surface of the panels. Prescribed voltages are statically applied to the piezoelectric actuators, inducing a prestress field which is responsible for the stress stiffening effects when coupled with the nonlinear strain components. Different geometric configuration, laminate stacking sequence, boundary conditions and curvatures are investigated. The study shows that mechanically strain-induced piezoelectric effect increases the rate of occurrence of flutter, stabilizing the plate. This stiffening of the structure is related to the voltage applied on the actuators and the geometrical parameters of the plate. Thus, one can control the occurrence of flutter speed by controlling the voltage applied and the proper design of the geometric properties of the panel and tailoring of the composite laminate.*

Keywords: *flutter;aeroelasticity;composite materials;finite elements;smart materials*

1. INTRODUCTION

The joint use of composite materials and piezoelectric materials in structures whose dynamic responses are important, especially in the aerospace business, is only natural. Composite laminates are thin because of their high stiffness/weight ratio. On the other hand, piezoelectric materials have small control authority and very good frequency response, what makes them ideal to be embedded or attached to structures undergoing appreciable dynamic movements. Moreover, the electromechanical coupling allows their use as both sensors and actuators.

In the recent years, a considerable number of studies on the aeroelastic analysis and flutter suppression of various aeroelastic systems have been reported in the open literature. Shin et al. (2006) analyzed the aeroelastic characteristics of supersonic cylindrical composite panels. The flutter properties were studied considering structural damping effects with the finite element method. Friedmann et al. (2004) presented a fundamental study of the aeroelastic behavior of hypersonic vehicles. Prakash and Ganapathi (2006) studied the influence of thermal environment on the supersonic flutter behavior of flat panels using the finite element method. Fazelzadeh and Hosseini (2007) investigated the aerothermoelastic behavior of supersonic rotating thin-walled beams. Using geometrically non-linear finite elements based on a layerwise theory, Oh and Kim (2009) researched the vibration characteristics and supersonic flutter of cylindrical laminated panels subjected to thermal loads.

Li et al. (2010) derived a state feedback suboptimal control law for the aeroelastic response and flutter suppression of a three-degree-of-freedom typical airfoil section based on the state-dependent Riccati equation method. Librescu et al. (2005) investigated the active aeroelastic control of 2D wing-flap systems to suppress the flutter instability and enhance the subcritical aeroelastic response to time-dependent external pulses. Librescu et al. (2005) further examined the dynamic aeroelastic response and the related robust control of aircraft swept wings exposed to gust and explosive type loads. Jegarkandi et al. (2009) researched the aeroelastic stability of a flexible supersonic flight vehicle using non-linear dynamics, nonlinear aerodynamics, and a linear structural model. Kwon et al. (2004) examined the non-linear aeroelastic characteristics of a wing with an oscillating control surface in transonic and supersonic regimes and observed the effects of rotational stiffness on the flutter properties.

Although there are many progresses in the aeroelastic analysis and flutter control of aircraft structures, in the above-mentioned works, the piezoelectric material which possesses the self-adaptive and active control abilities has not been fully exploited. Up to now, the piezoelectric material has been extensively used for the active vibration suppression of engineering structures (Baz and Ro., 1996; Sun and Tong., 2004; Kumar and Singh, 2009) energy harvesting (De Marqui et al., 2009) and pre-buckling enhancement of composite plates (de Faria and Donadon., 2010; de Faria et al., 2011).

ISSN 2176-5480

The inverse piezoelectric effect is used in this work, i.e., strains are induced through the application of voltages to the piezoelectric patches. The strains piezoelectrically induced generate a stress field over the composite laminate that, depending on a number of parameters which will be addressed, stiffens the laminate. This effect is achieved with minimal mass overhead since very small piezoelectric patches are seen to significantly alter the laminate stiffness for relatively low voltage levels. The objective is to obtain the governing dynamic equations of laminated curved panels with piezoelectric actuators attached and subject to aerodynamic loads whose effects are accounted for using the piston theory, applicable to supersonic flows, and the virtual work of the nonconservative aerodynamic pressure over the panels. These governing equations are then solved in the frequency domain by the finite element technique. The finite element employed is the *R16* (Bismarck, 1991) which has four nodes and four degrees of freedom per node. Instead of in-plane strains and displacements this element interpolates the Airy stress function which can be later eliminated from the system of matrix equations, resulting in a single FE equation in the nodal transverse displacements.

2. PROBLEM FORMULATION

The aeroelastic dynamic response of a composite cylindrical thin panel with piezoelectric patches perfectly bonded to its surfaces is investigated. Figure 1 depicts the configuration studied and the cylindrical coordinate system used in the analysis. The shell is considered to be thin with total thickness h and adequately modelled by Kirchhoff's assumptions. A supersonic flow with airspeed U_∞ along x is imposed on the panel. This type of formulation has been extensively used in the literature for the analysis of beams (Hanagud et al., 1992), rings (Lalande et al., 1995) and general shells (Pletner and Abramovich, 1997) with piezoelectric elements.

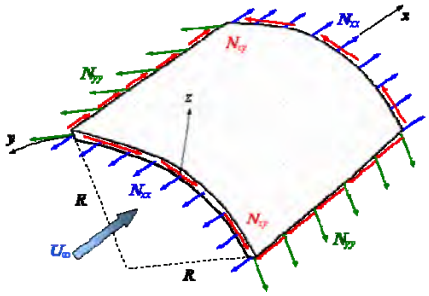

Figure 1. Curved cylindrical panel in the presence of supersonic flow

The electromechanical constitutive equations can be written as in Eq. (1), where it is assumed that the piezoelectric layers are polarized along the z direction (transverse direction perpendicular to the panel)

$$\bar{\boldsymbol{\sigma}} = \mathbf{C}\bar{\boldsymbol{\varepsilon}} - \mathbf{e}^T\mathbf{E} \qquad \mathbf{d} = \mathbf{e}\bar{\boldsymbol{\varepsilon}} + \boldsymbol{\xi}\mathbf{E}\,, \tag{1}$$

where **C** is the ply stiffness matrix, $\bar{\boldsymbol{\sigma}}$ is a vector of stresses, $\bar{\boldsymbol{\varepsilon}}$ is the strain vector, which includes linear and nonlinear components, **d** is the electric displacement, **E** is the electric field, **e** is the electromechanical coupling matrix, and $\boldsymbol{\xi}$ is the permittivity matrix. The cylindrical panel is modelled using classical thin-shell theory and von Kármán nonlinear strain × displacement relations. Accordingly, the in-plane displacements $\bar{u}(x,y,z)$ and $\bar{v}(x,y,z)$ are assumed to vary linearly through the thickness with respect to z and the transverse displacement $\bar{w}(x,y,z)$ is assumed independent of z. Thus the displacements are taken in the form

$$\begin{aligned}
\bar{u}(x,y,z) &= u(x,y) - zw_{,x}(x,y) \\
\bar{v}(x,y,z) &= v(x,y) - zw_{,y}(x,y) \\
\bar{w}(x,y,z) &= w(x,y)
\end{aligned} \tag{2}$$

where the field variables are u, v, w represent the mid surface displacements. Based on these expressions, the total strain ($\boldsymbol{\varepsilon}$), membrane strain ($\boldsymbol{\varepsilon}_m$) and curvature ($\boldsymbol{\kappa}$) vectors are given by

ISSN 2176-5480

$$\boldsymbol{\varepsilon} = \boldsymbol{\varepsilon}_m + z\boldsymbol{\kappa} = \begin{Bmatrix} u_{,x} + w_{,x}^2/2 \\ v_{,y} + w/R + + w_{,y}^2/2 \\ u_{,y} + v_{,x} + w_{,x}w_{,y} \end{Bmatrix} + z\begin{Bmatrix} -w_{,xx} \\ -w_{,yy} \\ -2w_{,xy} \end{Bmatrix} \tag{3}$$

where R is the cylindrical panel radius. Admitting that the electric potential (ϕ) varies linearly along the piezoelectric ply thickness and is constant in the plane

$$\phi(z) = \left(1 + \frac{z_k - z}{h_k}\right)\phi_k \quad , \quad z_k \le z \le z_{k+1} \tag{4}$$

where z_k is the position of the bottom surface of layer k in the thickness direction, h_k is the thickness of layer k and ϕ_k is electric potential on the bottom surface of layer k. Using Eq. (4), the electric field components E_x, E_y and E_z can be computed as

$$E_x = -\frac{\partial\phi}{\partial x} = E_y = -\frac{\partial\phi}{\partial y} = 0 \qquad E_z = -\frac{\partial\phi}{\partial z} = \frac{\phi_k}{h_k} \tag{5}$$

Given the strains in Eq. (3) and electric field in Eq. (5) the constitutive equation, Eq. (1), simplifies to

$$\boldsymbol{\sigma} = \bar{\mathbf{Q}}\boldsymbol{\varepsilon} - \mathbf{e}'E_z \qquad d_z = (\mathbf{e}')^T\boldsymbol{\varepsilon} + \xi_{33}E_z \ , \tag{6}$$

where $\bar{\mathbf{Q}}$ is the in-plane ply stiffness matrix in the structural coordinate system, d_z is the electric displacement z component , $\boldsymbol{\sigma} = \{\sigma_{xx} \ \ \sigma_{yy} \ \ \tau_{xy}\}^T$, $\boldsymbol{\varepsilon} = \{\varepsilon_{xx} \ \ \varepsilon_{yy} \ \ \gamma_{xy}\}^T$, and $\mathbf{e}' = \{ e_{31} \ \ e_{31} \ \ 0\}^T$. Vector $\mathbf{e}'$ is obtained through a transformation of the coordinate system when $e_{31} = e_{32}$; a valid assumption for transversely isotropic piezoelectric material (Nye, 1972). Laminate matrices $\mathbf{A}$, $\mathbf{B}$, $\mathbf{D}$ and stress resultant piezoelectric vectors $\mathbf{N}_p$, $\mathbf{M}_p$ are defined as

$$\begin{aligned} (\mathbf{A},\mathbf{B},\mathbf{D}) &= \int_{-h_p-h/2}^{h_p+h/2} (1, z, z^2)\bar{\mathbf{Q}}dz \\ (\mathbf{N}_p,\mathbf{M}_p) &= \int_{-h_p-h/2}^{h_p+h/2} (1, z)\mathbf{e}'E_z dz \end{aligned} \tag{7}$$

where h_p is the thickness of the piezoelectric layers assumed to be symmetrically placed on the top and bottom panel surfaces. Notice that the laminate matrices are affected by the stiffness of the piezoelectric layers. Accordingly, the integration limits $\pm(h_p + h/2)$ must be adjusted to reflect presence or absence of piezoelectric layers in the laminate, i.e., when there no actuator layers, $h_p = 0$. Moreover, $\mathbf{N}_p$, $\mathbf{M}_p$ are zero if no piezoelectric layers are present. The finite element method used to numerically solve the governing equations is based on energy principles. The kinetic energy of the system is

$$T = \frac{1}{2}\int_A \rho h\dot{w}^2 dA \tag{8}$$

where ρ is density, h is the total thickness and A is the cylindrical panel mid surface domain. Again, ρ and h must be adjusted to account for presence or absence of piezoelectric layers. The strain energy of the electromechanical system is (Reddy, 1997):

$$\begin{aligned} U = &\frac{1}{2}\int_V \boldsymbol{\varepsilon}_m^T\bar{\mathbf{Q}}\boldsymbol{\varepsilon}_m dV + \int_V z\boldsymbol{\varepsilon}_m^T\bar{\mathbf{Q}}\boldsymbol{\kappa}dV + \frac{1}{2}\int_V z^2\boldsymbol{\kappa}^T\bar{\mathbf{Q}}\boldsymbol{\kappa}dV \\ &-\int_V (\boldsymbol{\varepsilon}_m^T + z\boldsymbol{\kappa}^T)E_z\mathbf{e}'dV - \frac{1}{2}\int_V E_z^2\xi_{33}dV \end{aligned} \tag{9}$$

ISSN 2176-5480

where V is the volume of the panel. The membrane $\mathbf{N} = \{N_{xx} \;\; N_{yy} \;\; N_{xy}\}^T$ and moment $\mathbf{M} = \{M_{xx} \;\; M_{yy} \;\; M_{xy}\}^T$ stress resultants are defined as $\mathbf{N} = \mathbf{A}\boldsymbol{\varepsilon}_m + \mathbf{B}\boldsymbol{\kappa}$ and $\mathbf{M} = \mathbf{B}\boldsymbol{\varepsilon}_m + \mathbf{D}\boldsymbol{\kappa}$ leading, after integration through the thickness of Eq. (9) and use of Eq. (7), to

$$\begin{aligned} U = &\frac{1}{2}\int_A [\boldsymbol{\varepsilon}_m^T(\mathbf{N}-\mathbf{N}_p) + \boldsymbol{\kappa}^T(\mathbf{M}-\mathbf{M}_p)]dA \\ &-\frac{1}{2}\int_{-h_p-h/2}^{h_p+h/2} E_z^2 A\xi_{33} dA \end{aligned} \tag{10}$$

The virtual work δW of the aerodynamic loads corresponds to the work of the aerodynamic pressure distribution over the panel and is given by

$$\delta W = \int_A \Delta p \delta w dA = \int_A \frac{2q_\infty}{\sqrt{M^2-1}} \frac{\partial w}{\partial x} \delta w dA = \int_A \lambda \frac{\partial w}{\partial x} \delta w dA \tag{11}$$

where δw is the transverse virtual displacement, M is the Mach number, q_∞ is the free stream dynamic pressure and $\lambda = 2q_\infty/(M^2 - 1)^{1/2}$ (Bismarck, 1999). Equations (8), (10) and (11) can now be combined to write, according to Hamilton's principle

$$\begin{aligned} &\delta\int_{t_1}^{t_2}(T-U)dt + \int_{t_1}^{t_2}\delta W dt = \int_{t_1}^{t_2}\Bigg[\int_A \rho h\dot{w}\delta\dot{w}dA \\ &-\int_A \delta\boldsymbol{\varepsilon}_m^T(\mathbf{N}-\mathbf{N}_p)dA - \int_A \delta\boldsymbol{\kappa}^T(\mathbf{M}-\mathbf{M}_p)dA + \int_A \lambda\frac{\partial w}{\partial x}\delta w dA\Bigg]dt = 0 \end{aligned} \tag{12}$$

The linearized static equilibrium equations are obtained from Eq. (12) making $\partial w/\partial t = 0$ and disregarding the nonlinear strain components in $\boldsymbol{\varepsilon}_m$ from Eq. (3). The linearized membrane strains become $\boldsymbol{\varepsilon}_L = \{\, u_{0,x} \;\; v_{0,y} + w_0/R \;\; u_{0,y} + v_{0,x} \,\}^T$ where the subscript '0' has been attached to denote prestress computations. Thus, Eq. (12) becomes, for the prestress problem

$$\int_{t_1}^{t_2}\int_A \Big[\delta\boldsymbol{\varepsilon}_L^T(\mathbf{N}_0-\mathbf{N}_p) + \delta\boldsymbol{\kappa}^T(\mathbf{M}_0-\mathbf{M}_p) - \lambda\frac{\partial w_0}{\partial x}\delta w_0\Big]dAdt = 0 \tag{13}$$

Using divergence theorem one can obtain the prestress linearized static equilibrium differential equations

$$\begin{aligned} &(N_{0xx}-N_{pxx})_{,x} + (N_{0xy}-N_{pxy})_{,y} = 0 \\ &(N_{0xy}-N_{pxy})_{,x} + (N_{0yy}-N_{pyy})_{,y} = 0 \\ &(M_{0xx}-M_{pxx})_{,xx} + 2(M_{0xy}-M_{pxy})_{,xy} + \\ &(M_{0yy}-M_{pyy})_{,yy} - (N_{0yy}-N_{pyy})/R + \lambda w_{0,x} = 0 \end{aligned} \tag{14}$$

One can now investigate the dynamic movement of the cylindrical panel about the linearized static equilibrium configuration computed in Eq. (14). To this end the membrane (**N**) and moment (**M**) stress resultants in Eq. (12) are written respectively as $\mathbf{N} + \mathbf{N}_0$ and $\mathbf{M} + \mathbf{M}_0$ where now **N** and **M** represent small perturbations about the equilibrium state, just like the transverse displacement is $w + w_0$, w being a small perturbation about equilibrium w_0. Substituting the perturbed stress resultants into Eq. (12) and using the divergence theorem again the dynamic differential equations are

$$\begin{aligned} &N_{xx,x} + N_{xy,y} = 0 \\ &N_{xy,x} + N_{yy,y} = 0 \\ &M_{xx,xx} + 2M_{xy,xy} + M_{yy,yy} + (N_{0xx}-N_{pxx})w_{,xx} \\ &+2(N_{0xy}-N_{pxy})w_{,xy} + (N_{0yy}-N_{pyy})w_{,yy} \\ &-N_{yy}/R + \lambda w_{,x} = \rho h\ddot{w} \end{aligned} \tag{15}$$

ISSN 2176-5480

where Eqs. (14) have been used and nonlinear terms $N_{xx}w_{,xx}$, $N_{yy}w_{,yy}$, $N_{xy}w_{,xy}$ were neglected since **N**, **M** and w represent small perturbations. In Eq. (15) it is clear that $(N_{0xx} - N_{pxx})$, $(N_{0xy} - N_{pxy})$, $(N_{0yy} - N_{pyy})$ reflect the piezoelectric stresses, which coupled with $w_{,xx}$, $w_{,yy}$, $w_{,xy}$ produce the stress stiffening. In order to solve Eqs. (16), the Airy stress function F is defined as

$$N_{xx} = \frac{\partial^2 F}{\partial y^2} \qquad N_{yy} = \frac{\partial^2 F}{\partial x^2} \qquad N_{xy} = -\frac{\partial^2 F}{\partial x \partial y} \tag{16}$$

There are two types of bending-membrane coupling: material and geometrical. The first type happens when the laminate is nonsymmetric whereas the second is due to the panel natural curvature. When the material coupling is null **B** = **0** (symmetric laminate) and the membrane $\mathbf{N} = \{N_{xx} \;\; N_{yy} \;\; N_{xy}\}^T$ and moment $\mathbf{M} = \{M_{xx} \;\; M_{yy} \;\; M_{xy}\}^T$ stress resultants become $\mathbf{N} = \mathbf{A}\boldsymbol{\varepsilon}_m$ and $\mathbf{M} = \mathbf{D}\boldsymbol{\kappa}$. Assuming a symmetric laminate and substituting Eq. (16) in (15c) the new dynamic equation in the transverse direction is

$$\begin{aligned} &D_{11}w_{,xxxx} + 4D_{16}w_{,xxxy} + 2(D_{12} + D_{66})w_{,xxyy} + 4D_{26}w_{,xyyy} + D_{22}w_{,yyyy} + \\ &-(N_{0xx} - N_{pxx})w_{,xx} - 2(N_{0xy} - N_{pxy})w_{,xy} - (N_{0yy} - N_{pyy})w_{,yy} + \\ &N_{yy}/R - \lambda w_{,x} + \rho h\ddot{w} = 0 \end{aligned} \tag{17}$$

The problem is now formulated in terms of two variables: the transverse displacement w and the Airy stress function F. However, only one dynamic equation is available: Eq. (18). The missing dynamic equation comes from the imposition of the compatibility equations involving strains. Considering the linearized membrane strains $\boldsymbol{\varepsilon}_L$ one can write the compatibility equation as

$$\varepsilon_{xx,yy} + \varepsilon_{yy,xx} = \gamma_{xy,xy} + w_{,xx}/R \tag{18}$$

Neglecting the quadratic terms in $\boldsymbol{\varepsilon}_m$ inversion of $\mathbf{N} = \mathbf{A}\boldsymbol{\varepsilon}_L$ results in $\boldsymbol{\varepsilon}_L = \mathbf{A}^{-1}\mathbf{N} = \mathbf{A}^*\mathbf{N}$. which can be introduced into Eq. (18) to provide the missing dynamic equation

$$\begin{aligned} &A_{11}^* F_{,yyyy} - 2A_{16}^* F_{,xyyy} + (2A_{12}^* + A_{66}^*)F_{,xxyy} \\ &-2A_{26}^* F_{,xxxy} + A_{22}^* F_{,xxxx} - \frac{w_{,xx}}{R} = 0 \end{aligned} \tag{19}$$

3. NUMERICAL SOLUTION

Solution of the dynamic governing equations, Eqs. (17) and (19), is achieved using the finite element method where the Galerkin approach is used. Equation (17) is multiplied by δw, an arbitrary but kinematically admissible displacement satisfying the homogeneous geometric boundary conditions applicable to w, and later integrated over A. Similarly, Eq. (19) is multiplied by δF, an arbitrary variation satisfying the homogeneous geometric boundary conditions applicable to F, and later integrated over A. The weak form of the variational equation is thereby obtained and discretized using the R16 (Bismarck, 1991) element which has 8 degrees of freedom per node: w, $w_{,x}$, $w_{,y}$, $w_{,xy}$, F, $F_{,x}$, $F_{,y}$ and $F_{,xy}$. Within each element both w and F are interpolated with the C^1 Hermitian polynomials ($w = \Sigma L_i w_i$ and $F = \Sigma L_i F_i$) which leads to the following matrix equations,

$$\begin{aligned} &\mathbf{M}\ddot{\mathbf{w}} + \mathbf{K}_{ww}\mathbf{w} + \mathbf{K}_{wF}\mathbf{f} + \lambda\mathbf{A}\mathbf{w} + [(N_{0xx} - N_{pxx})\mathbf{K}_{Gxx} + \\ &(N_{0xy} - N_{pxy})\mathbf{K}_{Gxy} + (N_{0yy} - N_{pyy})\mathbf{K}_{Gyy}]\mathbf{w} = \mathbf{0} \\ &\mathbf{K}_{Fw}\mathbf{w} + \mathbf{K}_{FF}\mathbf{f} = 0 \end{aligned} \tag{20}$$

where **w** and **f** are the global vectors of degrees of freedom associated with displacement and stress function. The detailed computation of the matrices involved in Eq. (20) can be found in (Bismarck, 1999). The degrees of freedom relative to F can be easily eliminated since $\mathbf{f} = -(\mathbf{K}_{FF})^{-1}\mathbf{K}_{Fw}\mathbf{w}$ what gives

$$\mathbf{M}\ddot{\mathbf{w}} + [\mathbf{K}_{ww} - \mathbf{K}_{wF}\mathbf{K}_{FF}^{-1}\mathbf{K}_{Fw} + \lambda\mathbf{A} + (N_{0xx} - N_{pxx})\mathbf{K}_{Gxx} + (N_{0xy} - N_{pxy})\mathbf{K}_{Gxy} + (N_{0yy} - N_{pyy})\mathbf{K}_{Gyy}]\mathbf{w} = \mathbf{0} \tag{21}$$

Assuming that vector **w** is of the form $\mathbf{w} = \mathbf{w}_0 \exp(j\omega t)$, where ω is the vibration frequency of the structure, $\mathbf{w}_0$ is the amplitude vector and $j = \sqrt{-1}$, Eq. (21) becomes

ISSN 2176-5480

$$[-\omega^2\mathbf{M}+\mathbf{K}_{ww}-\mathbf{K}_{wF}\mathbf{K}_{FF}^{-1}\mathbf{K}_{Fw}+\lambda\mathbf{A}+(N_{0xx}-N_{pxx})\mathbf{K}_{Gxx}+(N_{0xy}-N_{pxy})\mathbf{K}_{Gxy}+(N_{0yy}-N_{pyy})\mathbf{K}_{Gyy}]\mathbf{w}_0=\mathbf{0} \quad (22)$$

Equation (22) defines the eigenvalue problem that governs the solution of the aeroelastic instability of cylindrical panels subject to piezoelectric actuation. In Eq. (24) **M** is the mass matrix, $\mathbf{K}_{ww} - \mathbf{K}_{wF}\,(\mathbf{K}_{FF})^{-1}\,\mathbf{K}_{Fw}$ is the stiffness matrix, **A** is the aerodynamic matrix, and $\mathbf{K}_{Gxx}$, $\mathbf{K}_{Gxy}$, $\mathbf{K}_{Gyy}$ are the geometric stiffness matrices induced by piezoelectric effect. It can be noticed that, when the piezoelectric load $\mathbf{N}_0 - \mathbf{N}_p$ and the freestream dynamic pressure are zero ($\lambda = 0$), ω represents the natural frequency of the panel. On the other hand, as λ increases, the values of ω change until, when λ reaches a critical value, the frequencies of two vibration modes coalesce. Further increases in λ lead to the appearance of complex conjugate frequencies for those modes that coalesced, characterizing unstable movement of the structure since the amplitude of the harmonic movement of the panel would increase without bounds. Physically, this condition means that oscillation will increase until failure or collapse of the structure. This critical value of λ represents the aeroelastic stability frontier of the panel. Mathematically, when modes coalesce the panel dynamics is described by

$$\mathbf{w} = \mathbf{w}_0 \exp[(\omega_R + j\omega_I)t] \quad (23)$$

where the real part of the complex frequency is responsible for the increase of the amplitude until structural collapse.

4. NUMERICAL RESULTS

The finite element model formulated was validated with known results on the aeroelastic frontier of composite panels. A boron-epoxy plate with 8 layers $[0/90]_{2s}$ was analyzed. The plate dimensions are 400 × 400 in and 8 in thickness. Mechanical properties are $E_1 = 31\times10^6$ psi, $E_2 = 2.7\times10^6$ psi, $G_{12} = 0.75\times10^6$ psi, $\nu_{12} = 0.28$ and $\rho = 0.192\times10^{-3}$ lb.s^2/in^4. Table 1 shows that the model developed delivers results which are comparable to those found in the literature.

Table 1 – Values of $\lambda_{cr}^{*} = \lambda_{cr}\, a^3/(E_2h^3)$ and $\omega_{cr}^{*} = \omega_{cr}\,(a^2/h)(\rho/E_2)^{1/2}$ for a fully clamped orthotropic boron-epoxy square plate

Source	λ_{cr}^{*}	ω_{cr}^{*}
Triangular element (8 ×8 mesh) (Lee and Cho, 1990)	471.00	46.89
Rectangular element (6 ×6 mesh) (Pidaparti and Yang, 1993)	472.00	46.80
Series (Srinivasan and Babu, 1987)	474.60	47.19
Method of integral equations (Srinivasan and Babu, 1987)	446.36	46.09
Rectangular element 16 DOF (4 ×4 mesh) (Bismarck, 1999)	452.54	46.09
Rectangular element 16 DOF (8 ×8 mesh) (present work)	479.60	47.07

Figure 2 shows the effect of applying voltages to the piezoelectric actuators on the mode coalescence of a simply supported 2024-T3 aluminum flat panel with $a = b = 0.4$ m and $a/h = 100$.

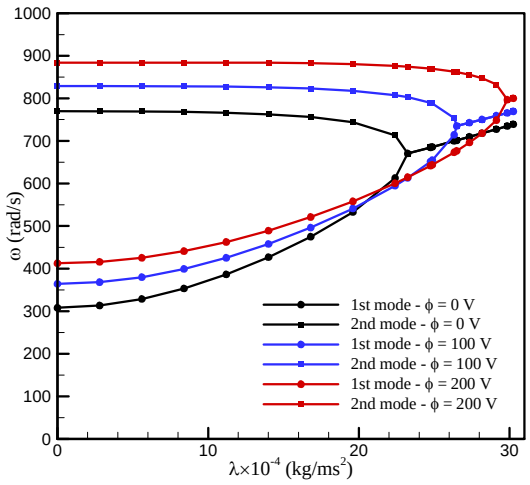

Figure. 2. Coalescence of the principal vibration modes when piezoelectric voltages are applied

ISSN 2176-5480

As seen in Fig. 2, application of voltages stabilizes the flat panel since the critical aerodynamic pressure increases. When ϕ = 50 V λ_{cr} increases 7% with respect to the ϕ = 0 V situation. Similarly, when ϕ = 100 V λ_{cr} increases 14%, when ϕ = 150 V λ_{cr} increases 21.2% and when ϕ = 200 V λ_{cr} increases 28.4%. Figures 3 and 4 show how λ_{cr}^{*} varies for a single layer boron-epoxy laminated flat panel when the lamination angle changes. It is noticed that the square panel either simply supported or clamped, provides the highest aeroelastic stiffness. λ_{cr}^{*} is reduced as the lamination angle θ increases from 0^o up to 90^o. The clamped square flat panel has a greater aeroelastic stiffness for all values of θ in comparison to the simply supported panel. The panel with r = 2, in both boundary conditions, has maximum λ_{cr^*} when $\theta = 30^o$. For $30^o < \theta \leq 90^o$ λ_{cr^*} decreases until its minimum value. As of $\theta = 65^o$ the simply supported laminate is stiffer than the clamped laminate.

In order to provide some metrics and evaluate the efficiency and cost of the inverse piezoelectric effects for all analysed cases, an inverse piezoelectric effectiveness parameter ε^* has been introduced. ε^* has been defined as a ratio between the relative increase in the critical dynamic parameter in respect to the normalized energy provided by the piezoelectric actuator, that is, $\varepsilon^* = \Delta\lambda_{cr} / \bar{U}\ \lambda_{cr}^0$ with $\Delta\lambda_{cr} = \lambda_{cr}^{\phi_i} - \lambda_{cr}^0$ and $\bar{U} = \left(CV^2/2\right)/\left(CV_{\max}^2/2\right) = \left(V/V_{\max}\right)^2$. C is the electrical capacitance of the piezoelectric actuator, V and $V_{\max}$ are the applied voltage and maximum voltage of the piezoceramic patch. $\lambda_{cr}^{\phi_i}$ and λ_{cr}^0 are the critical pressure parameters associated with ϕ_i (i=1 for 100 V and i=2 for 200 V) and $\phi = 0$ V, respectively. The piezo actuation system whose properties were used in this work is limited to $V_{\max}$ = 200 V by hardware.

Figures 5 and 6 depict the influence of lamination angle on the inverse piezoelectric effectiveness parameter for both boron-epoxy laminate simply supported and clamped cylindrical panels, respectively. The inverse piezoelectric effectiveness significantly increases as the lamination angle approaches $\theta = 90^o$ for both simply supported and clamped cylindrical panels. On the other hand, the inverse piezoelectric effectiveness is significantly reduced when θ approaches 0^o. Additional parametric studies including the effects of the shell curvature on flutter behavior of composite shells are provided in (de Almeida et al., 2012).

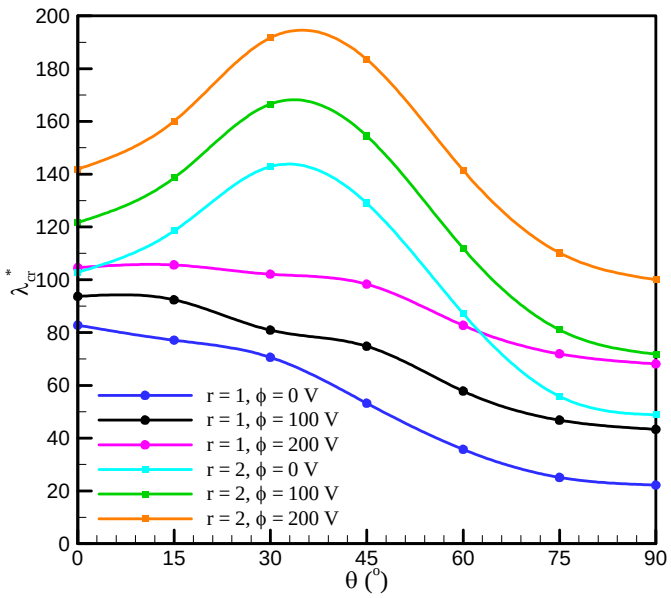

Figure 3. Influence of lamination angle on boron-epoxy laminated simply supported cylindrical panels with piezoelectric actuators charged

ISSN 2176-5480

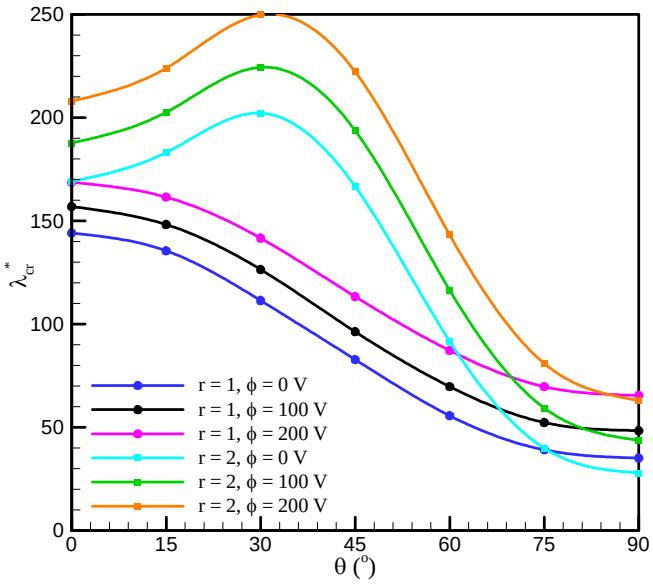

Figure 4. Influence of lamination angle on boron-epoxy laminated clamped cylindrical panels with piezoelectric actuators charged

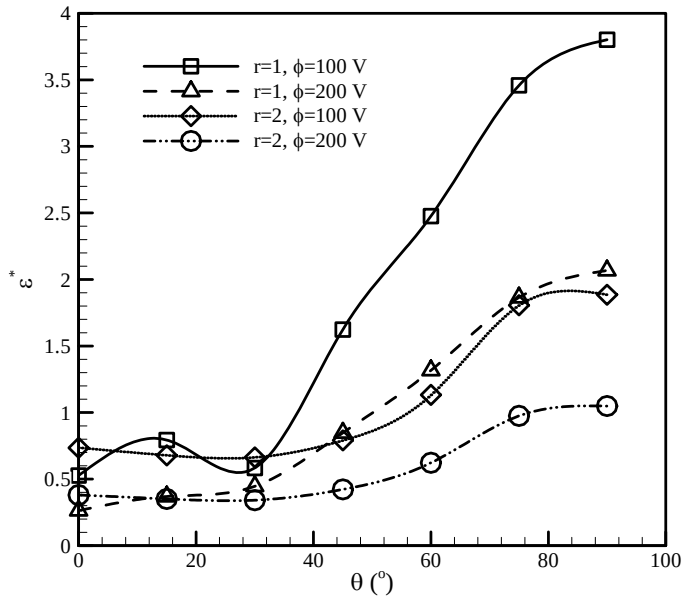

Figure 5. Influence of lamination angle on the inverse piezoelectric effectiveness parameter for boron-epoxy laminate simply supported cylindrical panels

ISSN 2176-5480

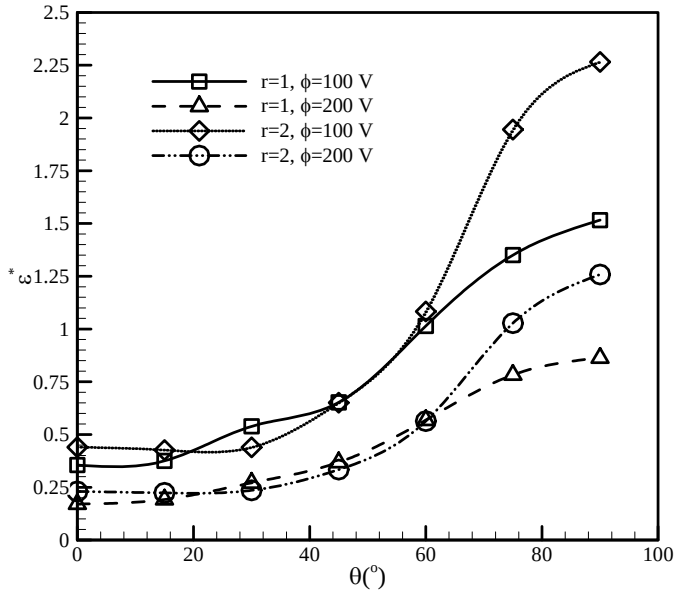

Figure 6. Influence of lamination angle on the inverse piezoelectric effectiveness parameter for boron-epoxy laminate clamped cylindrical panels

5. CONCLUSIONS

A significant increase of the aeroelastic stiffness in flutter may be achieved by means of piezoelectric actuators bonded to the vibrating structure such as an aeronautical composite panel. This device allows one to control the velocity and the frequency where flutter occurs. Although large patches of piezoelectric actuators cannot be found in the market, which could fully cover a aeronautical panel, large piezoelectric patches were considered for investigatory reasons, aiming at the understanding of the influence of geometric parameters (aspect ratio, curvature, lamination angles, thicknesses and boundary conditions) on the critical aerodynamic pressure. It was shown that a positive electrical charge stiffens the panel, increasing λ_{cr}. On the other hand, negative charges impair the panel stiffness, bringing down λ_{cr} and making the panel more vulnerable to flutter, i.e., it will become unstable at lower values of λ. This study proved that it is possible to control the airspeed where flutter occurs in aeronautical panels using piezoelectric actuators. The assessment conducted pointed to a large array of parameter combinations that may yield the best conditions for flutter aeroelastic instability control in aeronautical panels.

6. REFERENCES

Baz, A. and Ro, J., 1996. “Vibration Control of Plates with Active Constrained Layer Damping”. *Smart Materials and Structures*, (5):272-280.

Bismarck-Nasr, MN, 1991. “On the sixteen degree of freedom rectangular plate element”. *Computers & Structures*, 40(4): 1059–1060.

Bismarck-Nasr MN, 1999. *Structural Dynamics in Aeronautical Engineering. Reston.* AIAA Education Series.

De Marqui Jr, Erturk, Inamn D.J., 2009. “An Electromechanical Finite Element Model for Piezoelectric Energy Harvester Plates”. *Journal of Sound and Vibration*, (327):9-25.

de Almeida A.E., Donadon M.V., de Faria A.R., de Almeida S.F.M., 2012. “The effect of piezoelectrically induced stress stiffening on the aeroelastic stability of curved composite shells”, *Composite Structures*, 94:3601-3611.

de Faria, Alfredo R. , Oguamanam, Donatus C. D. Donadon, Mauricio V., 2011. “Prebuckling enhancement of imperfect composite plates using piezoelectric actuators”. *Journal of Applied Mechanics*, (78):031007-1.

de Faria, A. R., Donadon M.V. , 2010. “The use of piezoelectric stress stiffening to enhance buckling of laminated plates”. *Latin American Journal of Solids and Structures*, (7):167-183.

Friedmann, P.P., McNamara, J.J., Thuruthimattam, B.J. and Nydick, I., 2004. “Aeroelastic Analysis of Hypersonic Vehicles”, *Journal of Fluids and Structures*, (19):681-12.

Fazelzadeh, S.A. and Hosseini, M., 2007. “Aerothermoelastic Behavior of Supersonic Rotating Thin-Walled Beams made of Functionally Graded Materials”. *Journal of Fluids and Structures*, (23):1251-1264.

ISSN 2176-5480

Hanagud S, Obal MW, Calise AJ, 1992. “Optimal vibration control by the use of piezoceramics sensors and actuators”. *Journal of Guidance, Control, and Dynamics*, 15(5): 1199–1206.

Jegarkandi, M.F., Nobari, A.S., Sabzehparvar, M. and Haddadpour, H., 2009. “Aeroelastic Stability Consideration of Supersonic Flight Vehicle using Nonlinear Aerodynamic Response Surfaces”. *Journal of Fluids and Structures*, (25):1079-1101.

Kwon, H.J., Kim, D.H. and Lee, I., 2004. “Frequency and Time Domain Flutter Computations of a Wing with Oscillating Control Surface Including Shock Interference Effects”. *Aerospace Science and Technology*, (8):519-532.

Kumar, N. and Singh, S.P., 2009. “Vibration and Damping Characteristics of Beams with Active Constrained Layer Treatments under Parametric Variations”. *Materials and Design*, (30):4162-4174.

Lalande F, Chaudhry Z, Rogers CA, 1995. “Modeling considerations for in-plane actuation of actuators bonded to shell structures”. *AIAA Journal*, 33(7): 1300-1304.

Li, D., Guo, S. and Xiang, J., 2010. Aeroelastic Dynamic Response and Control of an Airfoil Section with Control Surface Nonlinearities. *Journal of Sound and Vibration*, (329):4756-4771.

Librescu, L., Na, S., Marzocca, P., Chung, C. and Kwak, M.K., 2005. Active Aeroelastic Control of 2-D Wing-Flap Systems operating in an Incompressible Flowfield and Impacted by a Blast Pulse. *Journal of Sound and Vibration*, (283):685-706.

Lee IN, Cho MH., 1990. “Flutter analysis of composite panels in supersonic flow”. In *Proceedings of the AIAA/ASME/ASCE/AHS/ASC 31st Structures, Structural Dynamics, and Materials Conference*, Long Beach, CA, 1990 (AIAA paper 90-1180).

Nye NY, 1972. *Physical Properties of Crystals: their representation by tensors and matrices*. Oxford University Press, London.

Oh, I.K. and Kim, D.H., 2009. ‘‘Vibration Characteristics and Supersonic Flutter of Cylindrical Composite Panels With Large Thermoelastic Deflections”. *Composite Structures*, (90):208-216.

Pletner B, Abramovich H., 1997. “Consistent methodology for the modeling of piezolaminated shells”. *AIAA Journal*, 35(8):1316-1326.

Pidaparti RMV, Yang HTY., 1993. “Supersonic flutter analysis of composite plates and shells”. *AIAA Journal*, 31(6): 1109-1117.

Prakash, T. and Ganapathi, M., 2006. “Supersonic Flutter Characteristics of Functionally Graded Flat Panels including Thermal Effects”. *Composite Structures*, (72):10-18.

Reddy JN, 1997. *Mechanics of Laminated Composite Plates: theory and analysis*. Boca Raton. CRC Press.

Srinivasan RS, Babu BJ., 1987. “Free vibration and flutter of laminated quadrilateral plates”. *Computers & Structures*, 27(2): 297-304.

Shin, W.H., Oh, I.K., Han, J.H. and Lee, I., 2006. “Aeroelastic Characteristics of Cylindrical Hybrid Composite Panels with Viscoelastic Damping Treatments”, *Journal of Sound and Vibration*, (296):99-16.

Sun, D. and Tong, L., 2004. “A Compressional-Shear Model for Vibration Control of Beams with Active Constrained Layer Damping”. *International Journal of Mechanical Sciences*, (46):1307-1325.

7. RESPONSIBILITY NOTICE

The author(s) is (are) the only responsible for the printed material included in this paper.